Progress In Electromagnetics Research C, Vol. 81, 89–99, 2018

Design of Circularly Polarized Tag Antenna with Artificial Magnetic Conductor for On-Body Applications

Jhih-Han Hong, Chien-Wen Chiu*, and Hwang-Cheng Wang

Abstract—This paper presents a circularly polarized tag on a 3×3 AMC structure to obtain longer read range for UHF RFID on-body applications. A modified T-matching transformer is employed to achieve conjugate matching with the Monza 4 microchip. To overcome the influence of lossy human body, a cross-dipole tag antenna is directly implemented on the phase-dependent AMC structure to achieve high gain and isolate the influence of the human body. Then, the tag is pasted on a lossy human model to investigate its performance. The study finds that the AMC can increase the antenna gain by 3.34 dB and help generate circularly polarized (CP) wave. The measured fractional bandwidth of impedance is 3.2% which can cover the UHF RFID bands of North America and Taiwan. The measured read range of the tag pasted on a human body reaches 15.7 meters when the reader has 4W EIRP, and the sensitivity of the microchip is -16.7 dBm.

1. INTRODUCTION

RFID (Radio Frequency Identification) is a non-contact automatic identification technology. An RFID system consists of many tags, a reader and a host computer to manage the information and service system. RFID technology has been widely applied in our life and industry, such as inventory, logistics, medical, transportation, trade, livestock, aviation, and education. RFID technology has gradually become more mature over the past decade. Nowadays, the convenience of RFID makes it a very important key technology for the Internet of Things (IOT) applications. The deployment of tags is required for the smart clothes in the application of IOT to the garment industry and clothing retail. UHF RFID tags for smart clothing are always pasted on objects which may be lossy media. However, the tag antenna is vulnerable to the influence of metal objects or lossy media such as water or a human body, even though the RFID technology has been used for many years. In order to tackle the serious interference caused by the lossy objects, researchers have proposed an artificial magnetic conductor (AMC) [1] to isolate the interference from the human body. However, the distance between the antenna and AMC is always very large for exciting circularly polarized waves. Our study focuses on putting the CP antenna directly on the artificial magnetic conductor (AMC), thereby reducing the overall thickness of the antenna.

Some scholars in AMC research area have proposed various miniaturization methods [2, 3]. Recently, the AMC has even been developed on soft substrates [4]. As the AMC is miniaturized, the resonance bandwidth becomes narrow. Therefore, a stacked AMC substrate was proposed in [5] to increase the bandwidth. Smart clothing has been rapidly developing in recent years Researchers have used diverse textile materials and analyzed the effects of bent AMCs [6, 7]. However, tags with AMC in the literature are mostly linearly polarized and seldom circularly polarized. Miscellaneous microstrip and patch antennas are often employed to excite circularly polarized waves on the AMC. When integrating a

Received 23 November 2017, Accepted 2 February 2018, Scheduled 11 February 2018

* Corresponding author: Chien-Wen Chiu (alexchiu@niu.edu.tw).

The authors are with the Department of Electronic Engineering, National Ilan University, No. 1, Sec. 1, Shennong Rd., Yilan City, Yilan County 26047, Taiwan.

patch antenna with AMC, the high impedance property of the AMC lets the distance between the AMC and the antenna have to be enlarged for exciting circularized waves [8, 9]. This approach can further increase antenna gain and bandwidth. Recently, some scholars have employed the design concept of the inductive RIS (reactive impedance surface) to compensate the electrically near field and thus control the coupling between the antenna and the AMC [10, 11]. This approach contributes to wide impedance matching and axial ratio (AR) bandwidth but miniaturizes the antenna size. In addition, a cross-dipole has been integrated with AMC to generate CP waves [12, 13]. The structure also has good antenna gain and radiation efficiency. However, the size and the thickness between the cross-dipole and AMC substrate are too large for use in RFID tags [9, 13]. So far, the study of AMC miniaturization still attracts a lot of attention [14, 15]. But there is only scarce research on how to reduce the thickness between the AMC substrate and the CP antenna.

In this study, a miniaturized cross-dipole antenna is successfully implemented on a 3×3 AMC substrate to generate CP waves. A T-matching transformer is employed to achieve conjugate matching with the microchip on an AMC substrate. Its AR fractional bandwidth of 3% is enough for operating in the UHF RFID band of North America. The measured read range is 17 meters in free space when the tag has a sensitivity of $-16.9\,\text{dBm}$. If the tag is directly put close to the human body, the results of the measured read range will change on various parts of the human body. Thus, the design is not stable. On the other hand, if the antenna has an AMC, the performance of the antenna near the human body will be very stable. When the tag with the AMC substrate is placed on a human body, the measured read range can be up to 15.7 meters. In order to further demonstrate the advantages of AMC, we also implement a circularly polarized tag without AMC and use it as a reference for performance comparison in terms of read range.

2. CP TAG ANTENNA DESIGN AND ANALYSIS IN FREE SPACE

The dimension of the CP tag before integrating with the AMC or putting near the human model is shown in Fig. 1. The CP tag antenna comprises two meandered dipole antennas which are individually designed in advance by referring to the method proposed in [16] and [17]. Phases of the input impedance for the two dipole antennas are set to $+45°$ and $-45°$, respectively. Therefore, the two dipoles have a $90°$ phase difference. The input impedances of the two arms are parallel connected [18] when they are combined and then modified. They are orthogonally combined to form a center-fed cross dipole and create CP waves. The cross-dipole antenna generates circularly polarized waves due to the orthogonal currents on the cross-dipole arms and $90°$ phase difference between the feeding points of the cross-dipole.

We apply a Monza4® microchip whose input impedance is $5 - j70\,\Omega$ to design the tag. It is not easy to excite CP waves and achieve conjugate matching between the antenna and the microchip at the

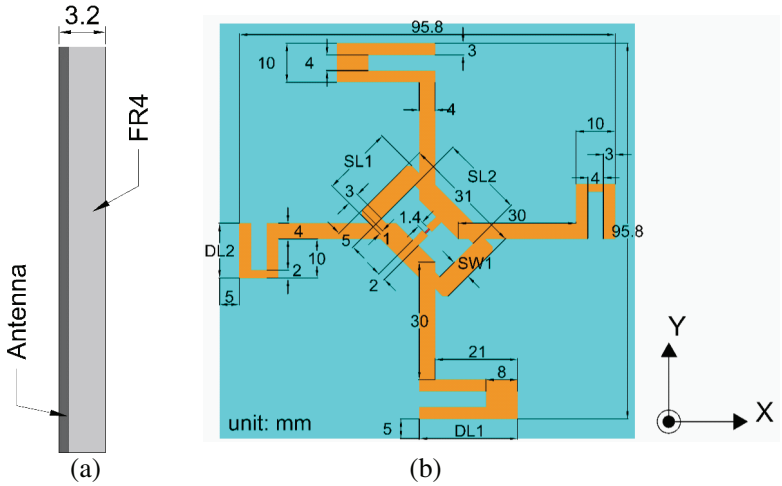

Figure 1. Geometry of the modified T-matching cross-dipole tag antenna (a) side view and (b) top view.

same time. Therefore, a modified T-matching is added to the feeding port of the antenna structure to make the impedance match with the input impedance of the tag. The T-transformer is adjusted so that the antenna impedance is conjugately matched with the input impedance of the Monza4® microchip. The lengths of the two meandered dipole antennas are made slightly different since it can help excite CP waves. However, the difference in size at the two ends of the antenna structure does not influence the resonant frequency too much since the current is zero at the two ends. The CP wave exciting is still preserved, and the AR bandwidth is wide enough for real applications.

The geometry of the antenna measures $105.8 \times 105.8\,\text{mm}^2$. The substrate thickness that we choose is 3.2 mm since it will be easier to generate circularly polarized waves than a thin one after adding an AMC in the back plane. Fig. 2 shows the simulated impedance and matching line. The modified T-structure transfers the impedance of the antenna for impedance matching. The parameter analysis of the T-matching structure is performed to make the input impedance match with that of the tag. Fig. 3 shows real part of the input impedance as a function of SW1. Fig. 4(a) and Fig. 4(b) show the imaginary part with respect to the change in SL1 and SL2, respectively. Finally, impedance matching is achieved when SL1 is 18 mm, SL2 is 21 mm, and SW1 is 5 mm.

Figure 5(a) shows the simulated axial ratio as a function of DL1, and Fig. 5(b) shows the axial ratio as a function of DL2. These parameters play important roles in generating CP waves when each arm of the antenna is less than one quarter wavelength. If the phase difference of the input impedance does not reach approximately 90° it will cause narrow AR bandwidth.

Figure 6 shows the simulated return loss obtained by the HFSS simulator compared with those obtained by the FEKO simulation tool. The impedance bandwidth ranges from 892 MHz to 932 MHz

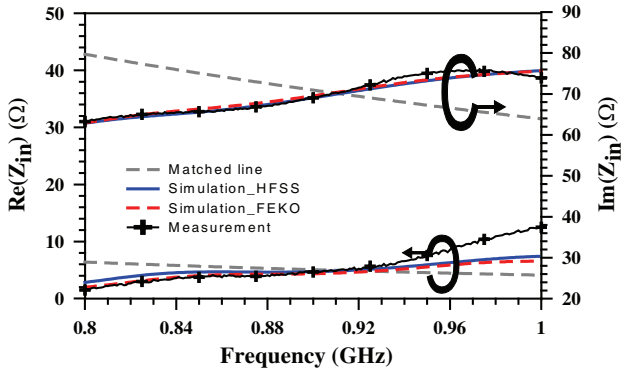

Figure 2. Simulated input impedance of the modified T-matching cross-dipole by HFSS and FEKO.

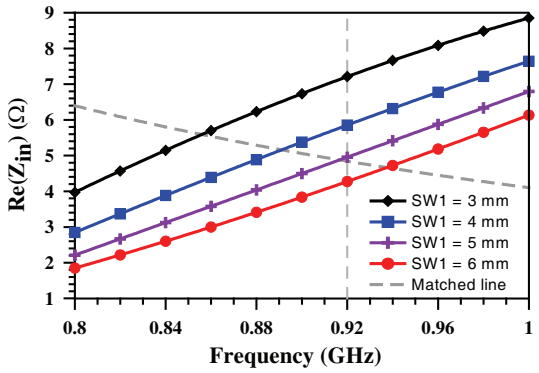

Figure 3. Simulated resistance of the antenna as a function of different SW1.

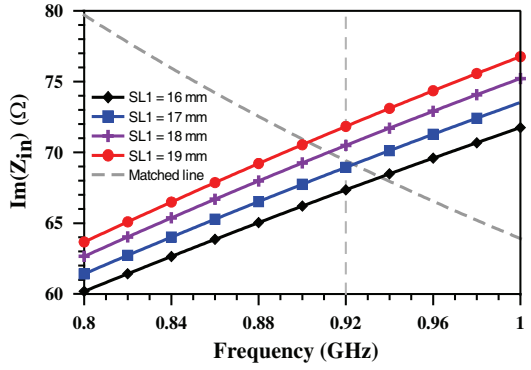

(a)

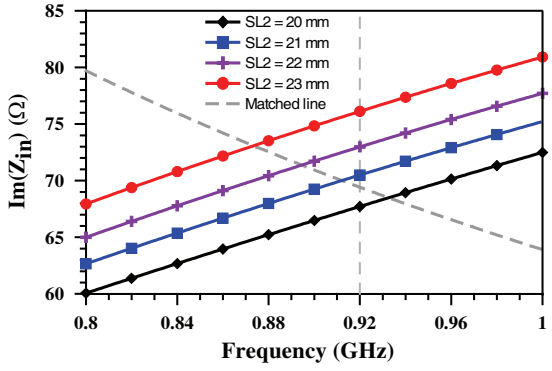

(b)

Figure 4. Simulated resistance of the antenna as a function of different values of (a) SL1 and (b) SL2.

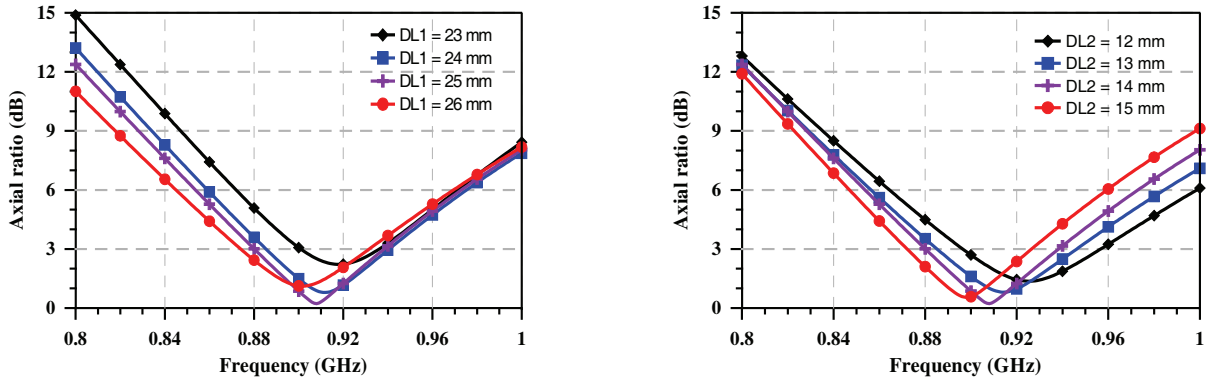

Figure 5. Simulated axial ratio of the antenna as a function of different values of (a) DL1 and (b) DL2.

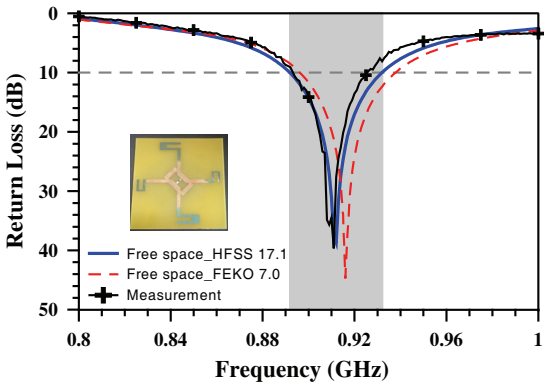

Figure 6. Calculated return loss of the modified T-matching cross-dipole by MATLAB.

Figure 7. Environment set-up for the impedance measurement of the cross-dipole tag antenna.

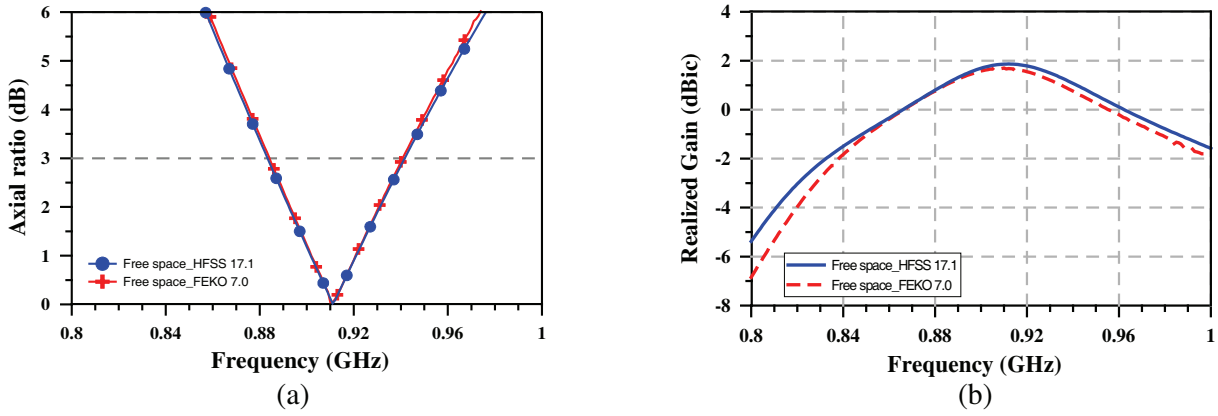

Figure 8. Simulated the modified T-matching cross-dipole: (a) axial ratio and (b) realized gain.

(4.4%). Impedance measurement of the tag is performed using a two-port VNA (Agilent 5071B) and a test fixture [19]. The configuration of the measurement set-up is illustrated in Fig. 7. The measured results show good agreement with the simulated results. Fig. 8(a) shows the simulated axial ratio with respect to operating frequencies. The AR bandwidth covers from 884 MHz to 941 MHz (6.2%). Fig. 8(b) shows the simulated realized gain by HFSS. It is verified by FEKO since the realized gain and axial ratio of a tag are not easy to measure. The maximum realized gain is about 1.86 dBic at 915 MHz. The predicted read range is about 12.5 meters if the EIRP power of the reader is 4 W, and the tag has a sensitivity of -16.9 dBm.

3. DESIGN OF CROSS-DIPOLE TAG ON THE AMC SUBSTRATE

AMC is a kind of infinitely periodic structure. The unit cell of the periodic structure is similar to a waveguide. The difference between the AMC model and the waveguide model is that the four sides of the square AMC are surrounded with mirror boundary conditions. The walls orthogonal to the electric field between two walls are set to PEC boundary. The walls orthogonal to the magnetic field between the other two walls are set to PMC boundary. The waveguide-like model simulates the infinitely periodic AMC structure [20]. A square waveguide model is always set up and then fed by a TEM wave at the feeding port of the model for simulation.

Figure 9 shows the rectangular unit cell of the periodic AMC structure. The thickness of the FR4 substrate is 3.2 mm. When the metal size of each square unit-cell AMC is $69 \times 69\,\text{mm}^2$, it can achieve the desired operating frequency. To generate a CP wave, the concept of phase-dependent AMC is applied [11]. When the gap between the metal patches is 1 mm and 2 mm along the X axis direction and Y axis direction, respectively, the AR bandwidth of the cross-dipole is the widest. Fig. 10 shows the simulated reflection phase on a rectangular unit cell of AMC. 0° reflection phase for X-polarization occurs at 903 MHz and 0° reflection phase for Y-polarization at 931 MHz.

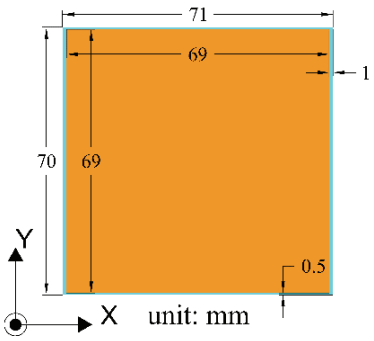

Figure 9. A unit cell of AMC structure.

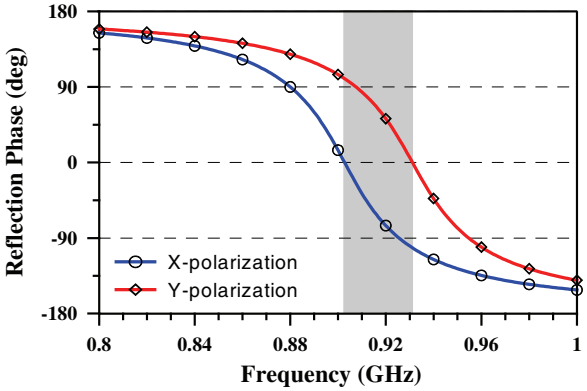

Figure 10. Simulated reflection phase on the square type AMC.

If the circularly polarized antenna is too close to a high impedance surface of the 3×3 AMC substrate, the strong coupling effect on the feeding point of the tag causes the conjugate matching to deteriorate. Therefore, we used a FR4 material with thickness 3.2 mm as substrate to support the antenna. The total thickness of the antenna and AMC is 6.4 mm, as shown in Fig. 11(a). The geometric configuration is shown in Fig. 11(b). The total size of the AMC substrate measures $211 \times 215 \times 3.2\,\text{mm}^3$.

According to the simulation test, the study finds that 3×3 AMC unit cells are enough to achieve maximum gain while preserving the AMC features. When the thickness of the cross-dipole antenna placed above the 3×3 AMC is 3.2 mm and $\varepsilon_r = 4.4$, loss tangent = 0.02, the original design of the antenna structure does not maintain the same performance as compared with that placed in the free space. The problem caused by coupling between the AMC surface and the antenna must be addressed Impedance matching must be performed again by modifying the T-matching transformer. The T-matching circuit is tuned to overcome the high impedance characteristics of AMC. The width of SW1 is increased to reduce the real part of the impedance and the lengths of DL1 and DL2 are adjusted to achieve a phase difference of 90° between the two cross-dipole arms. They satisfy the design conditions for exciting circularly polarized waves. In addition, the axial ratio bandwidth is the widest when the X-axis spacing between adjacent AMC metal sheets is increased to 2 mm. The simple T-matching transformer is sufficient to achieve conjugate matching with the microchip.

Figure 12 shows the simulated input impedance and the original match line. The T-matching structure of the cross-dipole on the AMC helps to conjugately match with the input impedance of the microchip, $5 - j70\,\Omega$. After the design is completed, the tag with the AMC is constructed to verify the simulated results. A test fixture as shown in Fig. 13 is utilized to accurately measure the impedance

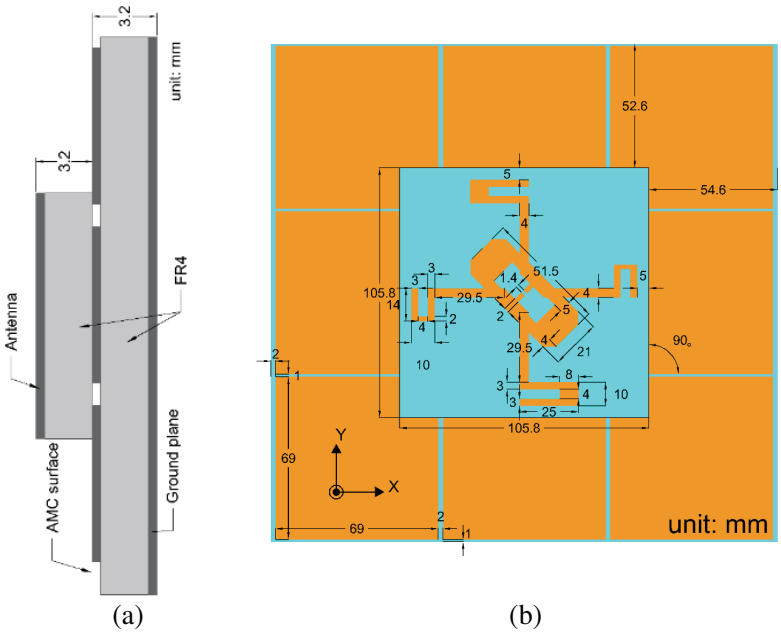

Figure 11. Geometry of the tag over the 3×3 AMC substrate, (a) side view and (b) top view.

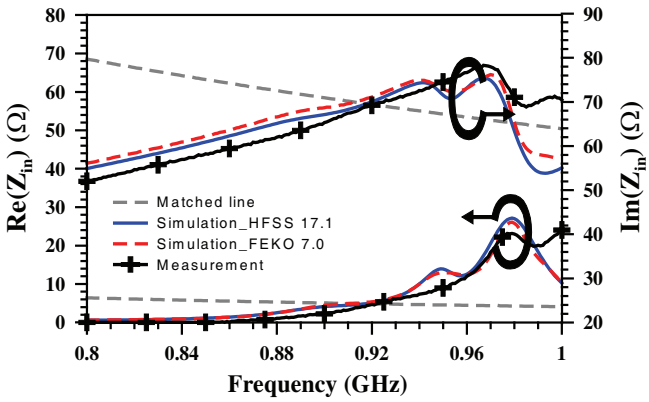

Figure 12. Simulated and measured input impedance of the tag on the 3×3 AMC substrate.

Figure 13. Impedance measurement of the cross-dipole tag together with the 3×3 AMC substrate.

for the verification of the simulated results. The measured impedance shows good agreement with the simulated result, as shown in Fig. 12. Fig. 14(a) shows the simulated and measured return loss of the tag on the AMC. The measured fractional bandwidth is about 2.5%, which covers from 905 MHz to 928 MHz. There is some discrepancy between the simulated results and the measured data because the large AMC substrate of $211 \times 215 \times 6.4\,\text{mm}^3$ is hard to fabricate accurately in the lab. The simulated AR bandwidth is 28 MHz (ranging from 903 MHz to 931 MHz, or 3%), as shown in Fig. 14(b). The result indicates that it is sufficient to cover the ISM RFID band for applications in North America. The figures also show the simulated results by HFSS compared with those by FEKO. The comparison confirms the validity of our simulation.

Figure 15 shows the radiation patterns in the XZ plane and YZ plane at 915 MHz. The study finds that the RHCP radiation field is symmetric. The shapes of the hemispherical pattern for RHCP and LHCP and the current distribution (not shown here) demonstrate that the cross-dipole antenna on the AMC generates excellent circularly-polarized waves. The simulated pattern results reveal that

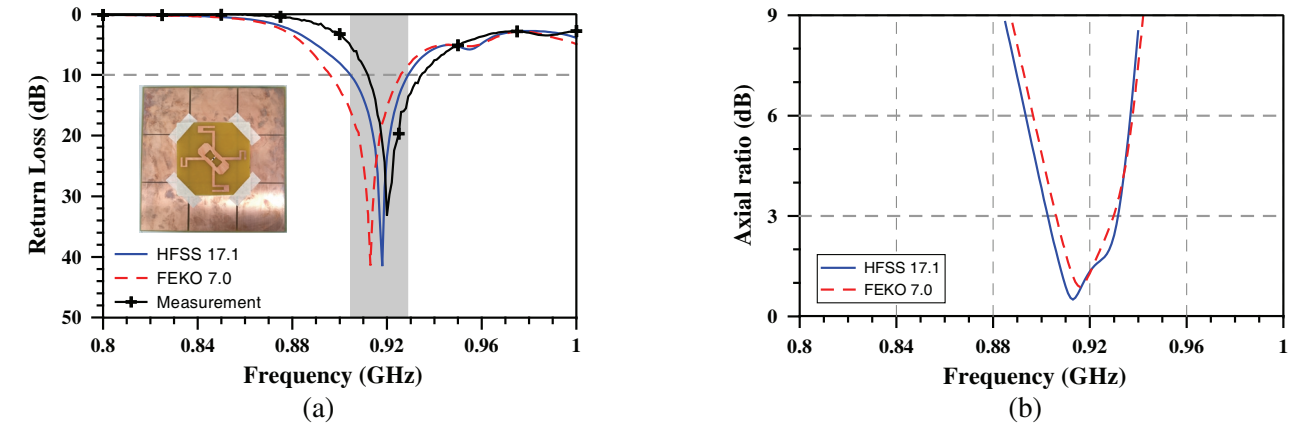

Figure 14. Simulated and measured (a) return loss and (b) axial ratio of the tag on the 3×3 AMC substrate.

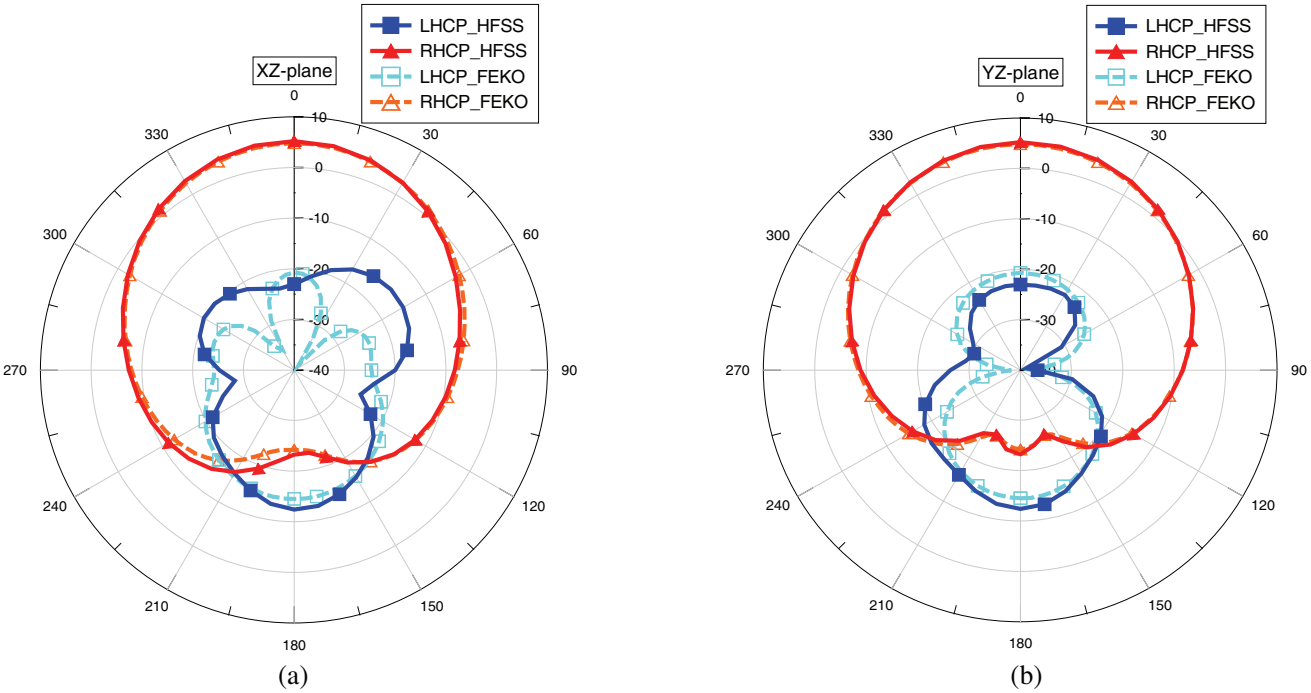

Figure 15. Simulated radiation patterns of the tag on the 3×3 AMC substrate, (a) XZ plane and (b) YZ plane.

the main beam is concentrated on the $+Z$ direction. The simulated beam width is about 68.65°. The maximum realized-gain is 5.13 dBic at 915 MHz. The antenna gain of the antenna with AMC is better than that of the original cross-dipole without AMC.

The predicted read range for the cross-dipole with AMC is over 18 meters which is calculated by the Friis formula. The practical tag with the antenna on the AMC is fabricated to measure the read rage. The measured read range for the cross-dipole with AMC achieves 17 m. The read range of the proposed antenna is greater than that of a linearly polarized dipole since the cross-dipole on the AMC is circularly polarized. Besides, the cross-dipole on the AMC shows immunity against the influence of lossy objects.

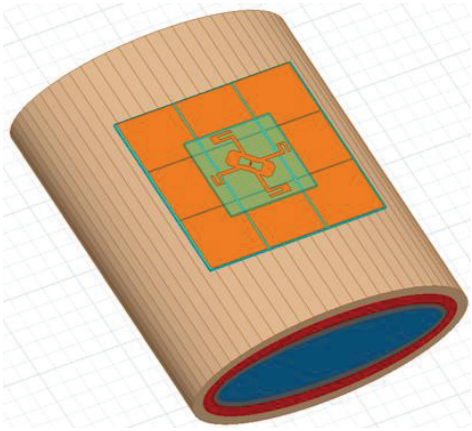

Figure 16. Simulation of the cross-dipole and a 3×3 AMC substrate on the human model.

4. TAG WITH THE 3×3 AMC SUBSTRATE ON THE HUMAN MODEL

Figure 16 shows an approximate human model for on-body antenna simulation and performance prediction. The human model consists of a stratified elliptical cylinder with four layers to model human torso. The height of the model is 400 mm, which is similar to the length of our torso. Details of the model parameters can be found in [21] or [22]. For a fair comparison, the cross-dipole on the FR4 substrate is 5.2 mm away from the human body but the cross-dipole with AMC is 2 mm away from the human body. This arrangement takes into account the thickness of the AMC. Antenna performance is compared in two different settings: on the human model and in the free space.

Figure 17 shows results of the realized gain and return loss for the tag with or without the AMC in the free space and on the human model. If the cross-dipole is close to the human body, the realized gain of the antenna without the AMC will become very poor, as shown in Fig. 17(a). The radiation efficiency of the cross-dipole on the human body becomes much lower than that of the cross-dipole in the free space. If an antenna designer wants to preserve antenna gain for on-body applications, he or she must improve the radiation efficiency of the antenna. The AMC helps to mitigate the human body effect. When the tag with the AMC is pasted on the human model, the realized gain still remains above 5 dBic. It is similar to the case in the free space. Fig. 17(a) also shows the realized gain of the optimized cross-dipole on the AMC plane compared with the cross-dipole on a PEC ground plane (GND). The result indicates that the antenna gain is conserved for the cross-dipole on the AMC plane but is deteriorated for the antenna put on the ground plane. The AMC plane or the PEC plane can reflect the wave so that they can avoid degradation caused by the lossy human body. However, the study finds that the antenna with the PEC plane does not preserve the benefit of wideband and suitable gain. The designed cross-dipole tag antenna on the AMC brings the realized gain up to 5.13 dBic. The antenna gain of the tag placed on the AMC is raised by over 3.34 dB compared to a circularly polarized dipole antenna in the free space.

Figure 17(b) shows the return loss for the tag with and without the AMC substrate. The study finds that the impedance bandwidth of the tag on the AMC substrate becomes narrow, as shown in Fig. 17(b). The impedance bandwidth becomes the narrowest as the antenna is put on the PEC plane. When the antenna on the AMC is pasted on the human model, the antenna retains good impedance matching. The impedance bandwidth ranges from 900 MHz to 930 MHz (3.2%) Fig. 18(a) shows comparison of the axial ratio for the tag with and without the AMC substrate. The study finds that the axial ratio bandwidth covers from 908 MHz to 938 MHz, (3.2%). The AMC isolates the interference from the human model, as shown in Fig. 18(a). Although the axial ratio band offsets slightly to high frequency in the UHF band of North America, this problem can be solved after fine tuning.

Figure 18(b) shows the radiation efficiency of the cross-dipole with and without AMC when they are close to the human model or in the free space. The result indicates that the radiation efficiency of the cross-dipole without AMC is more than 90% in the free space, but is less than 13.2% on the human

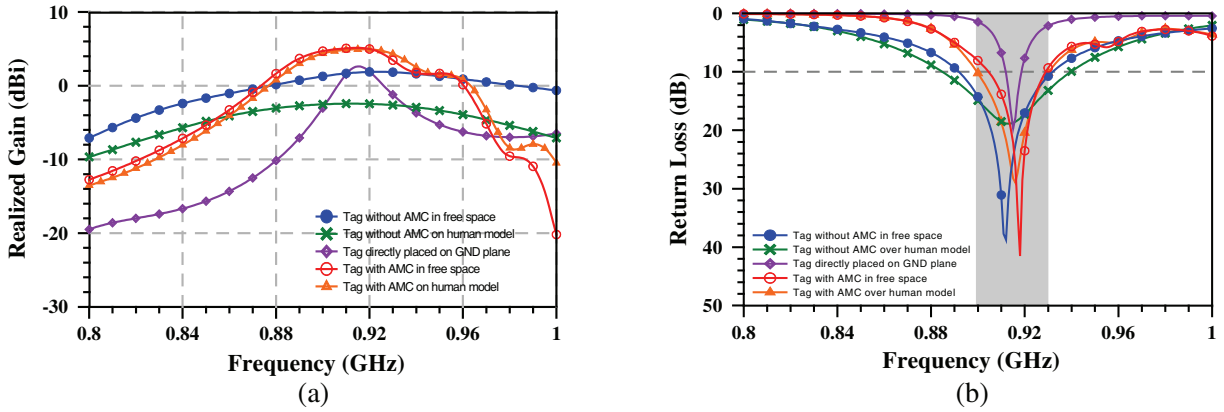

Figure 17. Simulated comparison in different environments, (a) realized gain and (b) return loss.

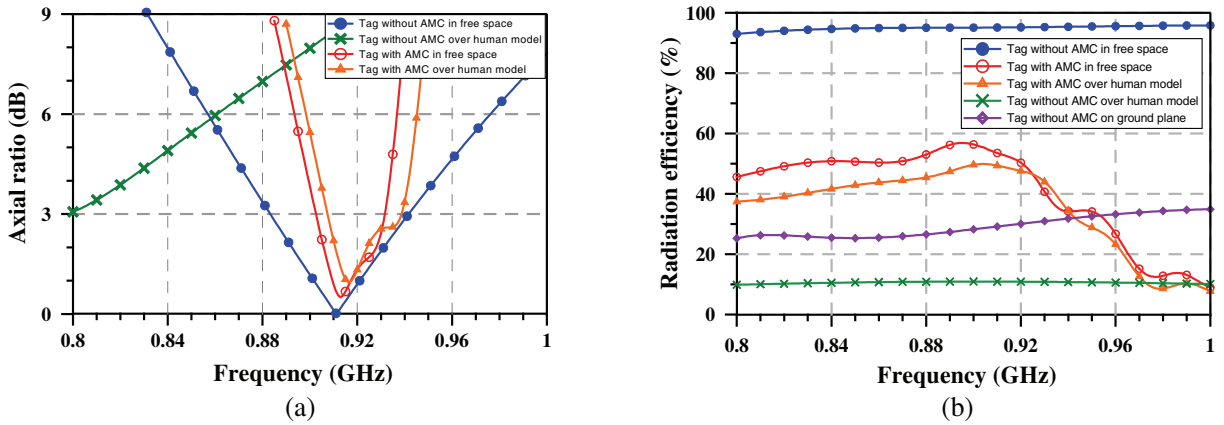

Figure 18. Simulated performance of the cross-dipoles in different environments: (a) axial ratio and (b) radiation efficiency.

Table 1. Performance comparisons.

Parameter \ Condition type	In the free space		On the human model	
	Tag without AMC	Tag with AMC	Tag without AMC	Tag with AMC
Realized gain	18.6 dBic	5.13 dBic	−2.44 dBi	5.01 dBic
Predicted reading range	12.3 m	18 m	5.34 m	17.7 m
Measured reading range	12.7 m	17 m	6 m	15.7 m
Radiation efficiency	95.6%	52%	13.1%	48%

body. This is due to the fact that the majority of the EM wave is absorbed by the human body. In contrast, the cross-dipole with AMC has a maximum radiation efficiency of 52%, which is much better than that of the cross-dipole without AMC. The study finds that the tag with AMC is not influenced by the body-proximity effects. The realized gain of the antenna with AMC near the human body is almost the same as that of the antenna in the free space. Since the AMC can shield the tag from the effect of the human body, the maximum radiation efficiency on the human body can be as high as 48%. Here, most loss comes from the lossy FR4 substrate. The efficiency can be higher if the substrate loss of the AMC and antenna is small. Furthermore, low-loss flexible substrate, such as textile or latex substrate

can replace the hard substrate for the AMC if the tag has to be designed directly on the human body for wearable RFID applications [7, 14, 23].

The performance comparison of the tags on different situations is summarized in Table 1. The left two columns list the predicted and measured read ranges in the free space. In the free space, the predicted read range is about 12.3 meters if the UHF RFID reader has 4W EIRP, and the sensitivity of the Monza microchip is −16.7 dBm. The measured read range can achieve over 12 meters since there is no polarization loss between the reader and the tag. Read ranges were measured with the tag pasted on the chest of a graduate student. The right two columns of the Table list the predicted and measured read ranges on the human body. The measured read range of the tag pasted on a human body reaches 15.7 meters. The read range of the tag on the AMC substrate is much longer than that of the cross-dipole without the AMC. The study finds that the read range and realized gain drop quickly due to the body adsorption effect if the tag without the AMC is directly pasted on the body. However, the tag with AMC is not influenced by the human body. Finally, the measured read range of the tag reaches over 15.7 m.

5. CONCLUSION

The paper presents a CP cross-dipole tag on a 3×3 AMC substrate and discussed the performance when it is put on the human model. The total size of the antenna system on the FR4 lossy substrate is $211 \times 215 \times 6.4\,\text{mm}^3$. The proposed T-matching transformer helps the tag overcome the high impedance surface of the phase-dependent AMC. The tag has been successfully designed and pasted on the 3×3 AMC substrate. The overall gain of the cross-dipole that comes from the contribution of the 3×3 AMC substrate increases by about 3.34 dB. The predicted read range can achieve 18 meters in the free space. When the cross-dipole with the AMC is close to the human model, the predicted read range is 17.7 meters. Its measured read range is about 15.7 meters when it is put on the human body. The measured fractional bandwidth of impedance is 3.2% so that the proposed tag can be used in the UHF RFID band of North America and Taiwan.

REFERENCES

1. Sievenpiper, D., L. Zhang, R. F. Broas, N. G. Alexopolous, and E. Yablonovitch, "High-impedance electromagnetic surfaces with a forbidden frequency band," *IEEE Transactions on Microwave Theory and Techniques*, Vol. 47, No. 11, 2059–2074, 1999.
2. Hadarig, R. C., M. De Cos, and F. Las-Heras, "Novel miniaturized artificial magnetic conductor," *IEEE Antennas and Wireless Propagation Letters*, Vol. 12, 174–177, 2013.
3. Coccioli, R., F.-R. Yang, K.-P. Ma, and T. Itoh, "Aperture-coupled patch antenna on UC-PBG substrate," *IEEE Transactions on Microwave Theory and Techniques*, Vol. 47, No. 11, 2123–2130, 1999.
4. Cos, M. E. de, Y. Álvarez, R. Hadarig, and F. Las-Heras, "Flexible uniplanar artificial magnetic conductor," *Proceedings of the 5th European Conference on Antennas and Propagation (EUCAP)*, 1218–1221, 2011.
5. Abu, M., E. E. Hussin, A. Othman, N. Yatim, F. Johar, and R. F. Munawar, "Design of stacked wafers AMC at 920 MHz for metallic object detection in RFID application," *IEEE Symposium on Wireless Technology and Applications (ISWTA)*, 236–239, 2013.
6. Zhu, S. and R. Langley, "Dual-band wearable textile antenna on an EBG substrate," *IEEE transactions on Antennas and Propagation*, Vol. 57, No. 4, 926–935, 2009.
7. Agarwal, K., Y. X. Guo, and B. Salam, "Wearable AMC backed near-endfire antenna for on-body communications on latex substrate," *IEEE Transactions on Components, Packaging and Manufacturing Technology*, Vol. 6, No. 3, 346–358, 2016.
8. Agarwal, K. and A. Alphones, "Design of compact circularly polarized microstrip antennas using meta-surfaces," *European Microwave Conference (EuMC)*, 1067–1070, 2013.
9. Tran, H. H. and I. Park, "A dual-wideband circularly polarized antenna using an artificial magnetic conductor," *IEEE Antennas and Wireless Propagation Letters*, Vol. 15, 950–953, 2016.

10. Dong, Y., H. Toyao, and T. Itoh, "Compact circularly-polarized patch antenna loaded with metamaterial structures," *IEEE Transactions on Antennas and Propagation*, Vol. 59, No. 11, 4329–4333, 2011.
11. Bernard, L., G. Chertier, and R. Sauleau, "Wideband circularly polarized patch antennas on reactive impedance substrates," *IEEE Antennas and Wireless Propagation Letters*, Vol. 10, 1015–1018, 2011.
12. Ta, S. X., I. Park, and R. W. Ziolkowski, "Circularly polarized crossed dipole on an HIS for 2.4/5.2/5.8-GHz WLAN applications," *IEEE Antennas and Wireless Propagation Letters*, Vol. 12, 1464–1467, 2013.
13. Ta, S. X. and I. Park, "Dual-band low-profile crossed asymmetric dipole antenna on dual-band AMC surface," *IEEE Antennas and Wireless Propagation Letters*, Vol. 13, 587–590, 2014.
14. Raad, H. R., A. I. Abbosh, H. M. Al-Rizzo, and D. G. Rucker, "Flexible and compact AMC based antenna for telemedicine applications," *IEEE Transactions on Antennas and Propagation*, Vol. 62, No. 2, 524–531, 2013.
15. Xue, C., H. Wang, X. Jiang, and Y. Huang, "A single-feed arrow-shaped circularly polarized antenna with unbalanced slotted artificial magnetic conductor for GNSS application," *IEEE MTT-S International Microwave Workshop Series on Advanced Materials and Processes for RF and THz Applications (IMWS-AMP)*, 1–3, 2016.
16. Deavours, D. D., "A circularly polarized planar antenna modified for passive UHF RFID," *IEEE International Conference on RFID*, 265–269, 2009.
17. Liu Y., Q. Liu, and J. Hu, "Novel circular polarization antenna for UHF RFID application," *2nd International Symposium on Instrumentation and Measurement, Sensor Network and Automation (IMSNA)*, 986–989, 2013.
18. Kraus, J. D., *Antennas*, 2nd Edition, New York, McGraw-Hill, 1988.
19. Qing, X., C. K. Goh, and Z. N. Chen, "Impedance characterization of RFID tag antennas and application in tag co-design," *IEEE Transactions on Microwave Theory and Techniques*, Vol. 57, No. 5, 1268–1274, 2009.
20. Mosallaei, H. and K. Sarabandi, "Antenna miniaturization and bandwidth enhancement using a reactive impedance substrate," *IEEE Transactions on Antennas and Propagation*, Vol. 52, No. 9, 2403–2414, 2004.
21. Tsai, M. C., C. W. Chiu, H. C. Wang, and T. F. Wu, "Inductively coupled loop antenna design for UHF RFID on-body applications," *Progress In Electromagnetics Research*, Vol. 143, 315–330, 2013.
22. Marrocco, G. "RFID antennas for the UHF remote monitoring of human subjects," *IEEE Transactions on Antennas and Propagation*, Vol. 55, No. 6, 1862–1870, June 2007.
23. Osman, M. A. R., M. K. A. Rahim, N. A. Samsuri, H. A. M. Salim, and M. F. Ali, "Embroidered fully textile wearable antenna for medical monitoring applications," *Progress In Electromagnetics Research*, Vol. 117, 321–337, 2011.